SCAND1 suppresses *CDC37* gene transcription by repressing MZF1

Taka Eguchi[1,2,*], Thomas L. Prince[1,3], Tien Manh Tran[2], Chiharu Sogawa[2], Benjamin J. Lang[1], and Stuart K. Calderwood[1,*]

[1]Divison of Molecular and Cellular Biology, Department of Radiation Oncology, Beth Israel Deaconess Medical Center, Harvard Medical School, Boston MA 02115 USA

[2]Department of Dental Pharmacology, Graduate School of Medicine, Dentistry and Pharmaceutical Sciences, Okayama University, Okayama 700-8525 Japan

[3]Department of Urology, Geisinger Clinic, Danville PA 17822 USA

Author Contributions: TE, TLP, and SKC conceptualized and designed the study. SKC and TE acquired funding. TLP and TE constructed materials. TE, TMT, CS, TLP, and BJL devised methodologies and performed experimentation. TE wrote the original manuscript. SKC, TLP and TE edited the manuscript. All authors reviewed the manuscript.

*To whom correspondence should be addressed:

Stuart K. Calderwood

3 Blackfan Circle CLS-610, Boston MA 02115 USA. Phone: +1-617-735-2947. Fax: +1-617-735-2814. E-mail: scalderw@bidmc.harvard.edu

Takanori Eguchi

2-5-1, Shikata-cho, Okayama 700-8558 Japan. Phone: +81-86-235-6662. Fax: +81-86-235-6664. E-mail: eguchi@okayama-u.ac.jp , eguchi.takanori@gmail.com

Running title: SCAND1 suppresses CDC37 by repressing MZF1

Abbreviations: CDC37, cell division control 37; CRPC, castration-resistant prostate cancer; EV, extracellular vesicle; HS, heat shock; HSE, heat shock element; HSF1, heat shock factor 1; HSP, heat shock protein; MZF1, myeloid zinc finger 1; NEPC, neuroendocrine prostate cancer; SCAN, SREZBP-CTfin51-AW1-Number 18 cDNA.

Peer-reviewed version available at Cancers 2019, 11, 792; doi:10.3390/cancers11060792

Abstract

Cell division control 37 (CDC37) increases the stability of HSP90 client proteins and is thus essential for numerous intracellular oncogenic signaling pathways, playing a key role in prostate oncogenesis. Notably, elevated expression of CDC37 was found in prostate cancer cells, although the regulatory mechanisms through which CDC37 expression becomes increased are unknown. Here we show both positive and negative regulation of *CDC37* gene transcription by two members of the SCAN transcription factor family- MZF1 and SCAND1, respectively. Consensus DNA-binding motifs for myeloid zinc finger 1 (MZF1 / ZSCAN6) were abundant in the *CDC37* promoter region. MZF1 became bound to these regulatory sites and *trans*-activated the *CDC37* gene whereas MZF1 depletion decreased CDC37 transcription and reduced tumorigenesis of prostate cancer cells. On the other hand, SCAND1, a zinc-fingerless SCAN box protein that potentially inhibits MZF1, accumulated at MZF1-binding sites in *CDC37* gene, negatively regulated *CDC37* gene and inhibited tumorigenesis. SCAND1 was abundantly expressed in normal prostate cells but was reduced in prostate cancer cells, suggesting a potential tumor suppressor role of SCAND1 in prostate cancer. These findings indicate that CDC37, a crucial protein in prostate cancer progression, is regulated reciprocally by MZF1 and SCAND1.

Keywords: SCAN zinc-finger, SCAND1, CDC37, MZF1, prostate cancer

Peer-reviewed version available at Cancers 2019, 11, 792; doi:10.3390/cancers11060792

Introduction

The cell division control 37 (CDC37) protein plays a fundamental role in chaperoning the protein kinase family and participates in cancer by maintaining the activity of protein kinases involved in cell proliferation and transformation. These include tyrosine kinases such as Src [1], and serine/threonine kinases in the Raf-ERK pathway [2], Akt [3], the inhibitor of NF-κB kinase (IKK) [4], and cyclin-dependent kinase 4 (CDK4) [5-7]. CDC37 functions primarily in a complex with heat shock protein 90 (HSP90) to mediate the 3-dimensional folding and structural integrity of client proteins kinases [1,8,9]. CDC37 is particularly significant in prostate cancer as its overexpression leads to prostate carcinogenesis in transgenic mice [10-12]. It has been suggested that the high levels of oncogenic proteins present in most cancers make them dependent on molecular chaperones, a state referred to as "chaperone addiction" [13,14]. Thus, because of their large protein clienteles, the CDC37-HSP90 axis offers a critical target for inactivating multiple oncogenic pathways [13,14]. Consequently, the inhibition of HSP90 in cancer is currently a major area of research [14,15]. However, less is known regarding the regulation of CDC37 expression in cancer and we have addressed this deficiency in this study.

Examination of the *CDC37* 5' upstream region and introns indicated multiple consensus sequences that are potentially bound by the transcription factor Myeloid Zinc Finger 1 (MZF1, a.k.a. ZSCAN6, ZNF42, ZFP98), consistent with a previous study [16]. We recently reported that frequent amplification of MZF1 was observed in human cancers, further suggesting an oncogenic role for this factor [17]. Early studies showed that MZF1 might play roles in stemness and in the differentiation of hematopoietic stem cells and indicated its involvement in myeloma [18]. MZF1 was shown to participate in the malignant properties of several major solid tumors, including breast [19,20], lung [21], liver [22], head

and neck [23], skin [24], endometrium [25], colorectal, and cervical cancer [26]. MZF1 protein structure is composed of an N-terminal SCAN domain, a linker region, and a C-terminal DNA binding domain that contains 13 repeats of zinc finger (ZF) motifs and is a member of the SCAN zinc finger (SCAN-ZF) family [17,27]. The SCAN domain is leucine-rich oligomerization domain and is highly conserved in the SCAN-ZF family, which is composed of more than 50 family members [28-30]. Zinc fingerless SCAN domain-only proteins also exist [27]. SCAND1 is a SCAN domain-only protein that has been shown to bind MZF1 and other SCAN-ZF family members. SCAN domain-only proteins have been suspected to be suppressors of intact SCAN-ZF transcriptional activity [27,28]. This possibility however has remained experimentally untested. Furthermore, we have tested the hypothesis that the relationship between MZF1 and SCAND1 regulates CDC37 expression and thereby cancer growth.

In this report we have, for the first time, characterized the *CDC37* gene promoter and determined that MZF1 indeed increases *CDC37* expression, while SCAND1 represses CDC37 expression. Our findings provide insight into how MZF1-driven *CDC37* expression promotes cancer progression and how SCAND1 functions as a potential tumor suppressor by repressing *CDC37*.

Peer-reviewed version available at Cancers 2019, 11, 792; doi:10.3390/cancers11060792

Results

Elevated expression of CDC37 is caused by MZF1 in prostate cancer.

We first compared the expression levels of CDC37 between prostate cancer cell lines DU-145 and LNCaP, a castration-resistant prostate cancer (CRPC) cell line PC-3, and normal prostate cell line RWPE-1. CDC37 levels in the prostate cancer cells (PC-3, LNCaP, and DU-145) were higher than that of the normal cell line (Fig 1A). CDC37 levels in PC-3 cells were higher than that of the other prostate cancer cells in both confluent and growing conditions (Fig 1A).

Although there are several possible mechanisms for the elevation in CDC37 expression in prostate cancer, in the present study we have focused on transcriptional regulation as the most immediate level of control. To determine potential *cis*-acting regulatory elements in the gene, we analyzed the DNA sequence around *CDC37* gene, between the -3.6kbp position and +2kbp position counted from the transcription start site (TSS) and found numerous consensus MZF1 binding sequences (Fig S1).

To query increased CDC37 level in PC-3 shown in Fig 1A, we next examined MZF1 expression and localization. MZF1 localized in nuclei in PC-3 but in the cytoplasm in PNT2 (Fig 1B), suggesting that both expression and nuclear localization of MZF1 could be involved in the increased CDC37 level in PC-3 cells. Additionally, nuclear bodies of MZF1 (designated MZF1-NBs) were seen in PC-3 but not in prostatic normal PNT2 cells, although the significance of the MZF1-NB is currently not known (Fig 1 B, C). Moreover, MZF1 overexpression led to increases in CDC37 levels in PC-3 cells (Fig 1D) while siRNA-mediated knockdown of MZF1 lowered CDC37 mRNA and protein levels (Fig 1 E, F). A role for MZF1 in CDC37 transcription was thus suspected.

To investigate the potential clinical significance of MZF1 regulation of CDC37, we next examined the co-expression correlation of MZF1 and CDC37 in prostate cancer patient-

Peer-reviewed version available at Cancers 2019, 11, 792; doi:10.3390/cancers11060792

derived tumor samples. Co-expression correlation was found between MZF1 and CDC37 in CRPC patient samples (Spearman's rank correlation score: 0.78) and in prostate adenocarcinoma patient samples (Spearman's correlation: 0.41). We next examined MZF1 and CDC37 expression correlation with the prognosis of prostate cancer patients. High expression of MZF1 (P=0.0287) and CDC37 (P=0.0182) were correlated with poor prognosis of patients suffering from prostate cancer (Table 1).

These data indicated MZF1 to be a potentially causal transcription factor for elevated expression of CDC37 in prostate cancer.

SCAN zinc finger protein MZF1 directly *trans*-activates the *CDC37* gene.

We next queried whether the SCAN zinc finger MZF1 could directly *trans*-regulate the *CDC37* gene through direct binding to *cis*-elements (MZF1 binding sequences) abundantly found in the *CDC37* 5'-upstream region. We examined the activities of *CDC37* promoter-driven luciferase reporter constructs containing different deletion mutants of the 5' region and examined potential trans-regulation by MZF1 and its SCANless truncation constructs of the factor (Fig 2 A, B). The full-length native MZF1 markedly increased *CDC37* promoter activities (of 3.6k, 950, 500/utr, 500, 202/utr) (Fig 1C). The SCANless mutant slightly increased *CDC37* promoter activities (of 500/utr, 500, 202/utr) but the transcriptional activity being much reduced compared with SCAN-containing native MZF1. These data indicated that SCAN oligomerization domain is essential for the transcriptional activity of MZF1. It is notable that the 202/utr reporter was more potent in trans-activation compared to other constructs, suggesting the presence of potential inhibitory motifs upstream of the 202 sequence. We next examined whether the overexpressed MZF1 (with Flag-tag) could directly bind to *cis*-elements in the genomic *CDC37* promoter region. MZF1 was detected by immunoblot in the

Peer-reviewed version available at Cancers 2019, 11, 792; doi:10.3390/cancers11060792

crosslinked chromatin fraction and potentially post-translational modification forms (upshift) and potential trimer were detected in the chromatin (Fig 2D). The overexpressed MZF1 occupied genomic *CDC37* promoter regions (-0.4k and -1.8k regions that contain MZF1-binding sites) further indicating that the *CDC37* gene is regulated by MZF1 binding to these MZF1 binding sites in prostate cancer (Fig 2E).

These data indicate that MZF1 directly *trans*-activates *CDC37* gene through direct binding to the *CDC37* promoter region and the SCAN domain-mediated trimerization is essential for full transcriptional activity of MZF1.

The Zinc-fingerless SCAND1 factor suppresses *CDC37* gene and tumorigenesis of prostate cancer

The SCAN-ZF family consists of more than 50 members and contains a few potentially inhibitory zinc fingerless members such as SCAND1. We hypothesized that SCAND1 could repress *CDC37* gene transcription through oligomerizing with SCAN-ZF proteins such as MZF1. Notably, SCAND1 is highly expressed in normal prostate compared to the other tissues (http://biogps.org/#goto=genereport&id=51282). We found SCAND1 to be expressed in normal prostate cells while its levels were reduced in prostate cancer PC-3 and DU-145 cells (Fig 3A), suggesting that SCAND1 expression declined along with prostate oncogenesis. Overexpression of SCAND1 led to lowered CDC37 levels in PC-3 cells (Fig. 3B).

To determine whether SCAND1 and a SCAN-only construct derived from MZF1 could regulate *CDC37* promoter constructs, we next carried out co-transfection and reporter assays. SCAND1 and SCAN-only constructs (SCAN and SCAN+linker) derived from truncation of MZF1 significantly repressed *CDC37* promoter activities (1.3k/utr, 500/utr, 202/utr) in PC-3 cells (Fig 3E). We also confirmed that the native MZF1 protein activated the CDC37 promoter

Peer-reviewed version available at Cancers 2019, 11, 792; doi:10.3390/cancers11060792

whereas the SCANless mutant had little effect.

We next hypothesized that SCAND1, although lacking ZF domains might be able to associate indirectly with MZF1-binding sites in genomic CDC37 promoter regions, perhaps through SCAND1-SCAN domain of MZF1 interaction. The overexpressed SCAND1 was detected in chromatin in PC-3 as monomer of the expected molecular weight. We also observed potential dimer and higher molecular weight forms in the crosslinked chromatin, suggesting higher oligomerization of SCAND1 on chromatin that might be consistent with a powerful repressor role (Fig 3F). The overexpressed SCAND1 (with Flag-tag) occupied the *CDC37* promoter region (-1.8k and -0.4k regions that we showed to contain MZF1-binding sites) (Fig 3G). The SCAND1 occupancy of the CDC37 regulatory site (-1.8k) was evidently much higher in magnitude than observed with MZF1 and SCAN-only constructs of MZF1 as suggested by increased enrichment in the ChIP assay (comparing Figs 2E, 3G). These data indicated that SCAND1 could repress CDC37 gene powerfully through association with DNA sequences that we showed to bind MZF1. Therefore, our data indicate that while MZF1 positively regulates CDC37, SCAND1 negatively regulates transcription, a finding which could be crucial in mechanisms of prostate cancer progression.

We therefore hypothesized that, in this context, *MZF1* has an oncogenic influence while *SCAND1* may suppress tumorigenicity. To elucidate this possibility, we asked whether tumor initiation by prostate cancer PC-3 cells could be suppressed by SCAND1 expression and by depletion of MZF1. Indeed, SCAND1 suppressed tumorigenicity of PC-3 cells (Fig 3H). Depletion of MZF1 also lowered tumorigenicity of PC-3 cells.

Peer-reviewed version available at Cancers 2019, 11, 792; doi:10.3390/cancers11060792

Discussion

Our data therefore suggest a novel mechanism for prostate cancer regulation by MZF1 (Fig. 1). CDC37 is a crucial molecule in prostate cancer growth through its fostering of oncogenic kinases and our data strongly indicate that the chaperone is regulated by MZF1. We show that MZF1 binds to sites in the CDC37 promoter and strongly activates transcription, and crucially that MZF1 expression is tightly correlated with CDC37 levels in clinical prostate cancer (Figs 1, 2). The ability of an endogenous inhibitor, the zinc fingerless SCAND1 factor to bind the promoter and repress transcription of MZF1 suggests a potential mechanism for prostate tumor suppression (Fig. 3). These data suggest mechanisms whereby members of the SCAN transcription factor family can fine-tune prostate cancer growth by up- or down-regulating CDC37 transcription and thus decide the outcome of prostate tumorigenesis (Fig 4). It is likely that other MZF1 targets important in tumorigenesis may be regulated in a similar way [17], including oncogenes and pro-tumorigenic genes such as MYC [21], NCAD [31], YAP1 [32], TGF-beta [20], CTSB/L [33], MMP-14 [34], FOXM1 [35], CK17 [36], PAX2 [25], PRAME [24], DR5 [37], AXL [26,38], PKC-alpha [39,40], CD34 and c-Myb [18]. Besides, MZF1 might play key roles also in tumor microenvironment such as mesenchymal stem cell differentiation into cancer-associated fibroblasts [20]. However, MZF1 has also been shown to activate tumor suppressor genes such as FPN [41], NFKBIA [42], and SMAD4 [43]. In a more complex manner, MZF1 also plays transcriptional repressor roles on pro-tumorigenic genes such as MMP-2 [44] and IGF-IR [45]. Nevertheless, our data do not exactly define the mechanism through which SCAND1 represses MZF1 activity although direct co-occupation of the *CDC37* promoter appears to be involved (Fig. 3). MZF1 was shown to bind DNA as a homodimer or heterodimer with other SCAN domain proteins and recruit chromatin remodeling protein mDomino [46]. Our data pinpoint the importance of the SCAN domain, as the SCANless construct of MZF1 showed

much reduced transcriptional activity compared to the powerful activity of the native MZF1 (Fig. 3E). The SCAN domain is leucine-rich and mediates oligomer formation [17]. We found that MZF1 could form a higher order structure, potentially a trimer on chromatin (Fig. 2D). Therefore, it was indicated that SCAN domain of MZF1 is required for its oligomerization and thus for a full activity for *trans*-activation. We also observed up-shift bands of MZF1 as potential post-translational modifications required for MZF1 activity (Fig 2D). It has been reported that MZF1 could be phosphorylated by PAK4 in a SUMO-directed manner [47], CK2 [31], and ERK-1/2 [36]. It was also reported that loss of the nuclear pool of ubiquitin ligase CHIP/STUB1 unleashes the MZF1-cathepsin pro-oncogenic program [33]. Thus, upstream regulatory signals that modify specific amino acid residues of MZF1 have been recently clarified. However, little is currently known regarding the mechanisms whereby SCAND1 could repress transcription, although our data indicate that this may associate with the CDC37 promoter in oligomeric form at the site of MZF1 binding (Fig. 3).

Our studies on CDC37 are aimed ultimately at targeting this factor in cancer as an alternative to Hsp90. Numerous HSP90 inhibitors have been developed to target the abundant HSP90, which plays versatile oncogenic roles in many types of cancer [48]. Moreover, extracellular HSP90 and extracellular vesicle-associated HSP90 has been recently shown to play pro-tumorigenic roles [49-53]. However, it has been difficult so far to employ Hsp90 inhibitors at effective doses due to normal tissue toxicity. Depletion of CDC37 reduced prostate cancer cell growth and attenuated MEK-ERK signaling pathway and PI3K-Akt signaling pathway [11]. Moreover, overexpression of CDC37 triggered prostatic tumorigenesis [10]. Our studies therefore suggest that further study of the role of MZF1 and SCAND1 in CDC37 transcription may indicate a potential mechanism that may be targeted for inhibition of expression of the chaperone.

In conclusion, it was demonstrated that pro-oncogenic MZF1 and its antagonist SCAND1 coordinately regulate expression of CDC37, a factor that is essential for prostate cancer tumorigenesis. The SCAN domain is required for full transcriptional activity of MZF1 whereas SCAN-only factor SCAND1 powerfully associates with chromatin and represses tumorigenesis of prostate cancer cells.

Peer-reviewed version available at Cancers 2019, 11, 792; doi:10.3390/cancers11060792

Materials and Methods

Cell culture.

PC-3, DU-145, LNCaP, and RWPE-1 cells were obtained from ATCC. PC-3 was cultured in F-12K or RPMI 1640 medium containing 5% to 10% fetal bovine serum (FBS). DU-145 was cultured in DMEM containing 5 to 10% FBS. LNCaP was cultured in RPMI 1640 medium containing 5% to 10% FBS. RWPE-1 was cultured in Keratinocyte Serum Free Medium (Thermo Fisher Scientific, Waltham, MA) supplemented with bovine pituitary extract (BPE) and human recombinant epidermal growth factor (hEGF). PNT2 was obtained from Sigma and cultured in RPMI 1640 medium supplemented with 2 mM glutamine and 5% to 10% FBS. Normal human prostate epithelial cells were purchased from Lonza (Basel, Switzerland) and cultured in Prostate Epithelial Cell Basal Medium (Lonza) supplemented with BPE, hydrocortisone, hEGF, epinephrine, transferrin, insulin, retinoic acid, triiodothyronine, and GA-1000.

Molecular Cloning.

Genomic DNA was isolated from a buccal cell swab of a deidentified white male. The 3.6 kbp human *CDC37* promoter region was PCR amplified and subcloned into a pGL3-luciferase vector (Promega, Madison, WI) using *Kpn*I and *Bam*HI. Once the pGL3-3.6 kbp CDC37promo vector was made, the 1.3 kbp, 950 kbp, 500 bp, 247 bp and 202 bp fragments with and without the 116-bp 5'UTR were subcloned into pGL3 similar using the same restriction sites as above. Each entire promoter fragment clone was Sanger sequenced. The complete 3.6 kbp *CDC37* promoter sequence was aligned with human reference genome GRCh37.

Human MZF1 cDNA was subcloned from pOTB-MZF1 into pcDNA3-Flag vector via TOPO directional cloning (Thermo Fisher Scientific) and designated pcDNA3/Flag-MZF1. For

Peer-reviewed version available at Cancers 2019, 11, 792; doi:10.3390/cancers11060792

SCAN-only constructs, UGA stop codons were generated in the pcDNA/Flag-MZF1 via Quickchange mutagenesis and designated pcDNA3/Flag-C125/SCAN and pcDNA3/Flag-C252/SCAN+L. For SCANless, the cDNA of MZF1 zinc-finger domain was amplified via PCR and subcloned into pcDNA/V5 vector using TOPO-directional cloning and designated pcDNA/MZF1-V5/N252 (SCANless). Human SCAND1 (NM_033630) ORF clone with Myc-DDK C-terminal tag (RC200079) was purchased (Origene, Rockville, MD) and designated pCMV6-ScanD1-myc-Flag. pCMV-EGFP (NEPA Gene) was used as an overexpression control.

***In silico* analysis of promoters and gene bodies.**

Sequences of promoter regions and gene bodies of human *CDC37, HSP90AA1* and *HSP90AB1* were obtained from the Eukaryotic Promoter Database [54]. Binding sites for MZF1 were predicted using PROMO [55,56].

Luciferase Assay. Transient transfection and luciferase assays were performed as previously described [57]. Cells were cultured in 96-well plates. A plasmid (25 ng reporter, 100 ng effector) was transfected with 0.4 µl FuGENE HD (Roche, Basel, Switzerland) per well at a cell confluence level of 50-70%. The medium was changed at 16-20 hours after transfection. At 40-48 hours after transfection, 70 µl of the medium was aspirated, then 30 µl of Bright-Glo reagent (Promega, Madison, WI) was added and mixed by pipetting. Cells were incubated for 5 minutes at 37°C. The lysate (40 µl) was transferred to a 96-well white plate for measurement of luminescence.

siRNA.

The siRNA was designed based on siRNA design method of JBioS (Japan Bio Services, Saitama).

RNA duplex of 19-bp plus TT-3' overhangs in each strand was synthesized by Nippon Gene (Tokyo, Japan). For electroporation-transfection, total of 40 pmol siRNA was transfected to 1 to 5 x 10^5 cells. For reagent-transfection, cells were transfected with siRNA at the final concentration of 20-100 nM. Non-targeting siRNA was purchased from Nippon Gene (Tokyo, Japan). The designed sequences of siRNA were listed in Supple Table.

Transfection.

For ChIP assay and tumorigenesis assay, electroporation-mediated transfection was performed as described previously [50,58]. To optimize electroporation for each cell type, cells (1×10^5 to 1×10^6 cells), plasmid DNA (2 to 10 μg total) or siRNA (40 pmol total), and serum-free medium were mixed to 100 μl total in a green cuvette with 1-mm gap (NepaGene, Ichikawa, Tokyo) and set to NEPA21 Super Electroporator (NepaGene). Poring pulse was optimized between 100V and 300V for 2.5 or 5.0 msec pulse length twice with 50 msec interval between the pulses and 10% decay rate with + polarity, as shown in a supplemental figure. Transfer pulse condition was five pulses at 20V for 50 msec pulse length with 50 msec interval between the pulses and 40% decay rate with +/- polarity. After electroporation, cells were recovered in serum-contained media. PC-3 (5×10^5 cells) was electroporation-transfected with 10 μg plasmid DNA or 40 pmol siRNA with poring pulse at 175V for 2.5 msec pulse length twice and then cultured for 5 days and 1×10^6 cells were subcutaneously injected to each SCID mouse.

For the overexpression-ChIP assay, DU-145 (5×10^6 cells) was transfected with 15 μg of pcDNA/Flag-MZF1 or pCMV-GFP with poring pulse at 175 V for 5 msec pulse length twice, cultured for 4 days in a 15-cm dish, and then used for ChIP assay.

For western blot analysis with overexpression of MZF1 and SCAND1, PC-3 cells were transfected with pcDNA3.1(-), pcDNA/Flag-MZF1, and pCMV6-SCAND1-myc-Flag using FuGENE6 (Roche).

For qRT-PCR after MZF1 depletion, PC-3 cells were transfected with a mixture of MZF1-siRNA A, B, and C (SR305183, OriGene, Rockville, MD) or non-silencing siRNA (SR30004, OriGene) using Lipofectamine RNAi max (Thermo Fisher Scientific).

For depletion of MZF1 and western blotting, DU-145 cultured in 6-well plate was transfected with siRNA hMZF1-all-NM_003422-53 using Lipofectamine RNAi Max. The medium was replaced with a fresh one at 24 hours after the transfection. Cells were lysed at 48 hours after the transfection.

Chromatin.

For protein overexpression and chromatin immunoprecipitation assay, DU-145 cells (5 x 10^6 cells) were electroporation-transfected with pCMV6-ScanD1-myc-Flag, pcDNA3/Flag-MZF1, pcDNA3/Flag-SCAN, pcDNA/Flag-SCAN+L, and pCMV-GFP and then cultured for 3 days in 150-mm dishes. ChIP was done using SimpleChIP enzymatic chromatin IP kit with magnetic beads (Cell Signaling Technology). For optimization, chromatin DNA was sheared with MNase (0, 0.25, 0.5, 0.75, and 1 µl per reaction) and ultra-sonication at high- and low-power using Ultrasonic Homogenizer Smurt NR-50M (Microtec Nition) and analyzed within 2%-agarose gel electrophoresis. After the optimization, chromatin DNA was sheared with MNase (0.75 µl per reaction) and ultra-sonication at high-power. Overexpressed proteins in the chromatin fraction were analyzed by western blotting using anti-MZF1 antibody (Assay Biotechnology) and anti-SCAND1 antibody (ab64828, Abcam, Cambridge, UK). Anti-Flag M2 magnetic beads (Sigma) were used for ChIP.

Peer-reviewed version available at Cancers 2019, 11, 792; doi:10.3390/cancers11060792

DNA was purified from the eluate and from 1% and 10% input chromatin using QIA-Quick DNA purification kit (Qiagen, Hilden, Germany) and eluted within 50 µl of ddH_2O. The purified DNA (3-5 µl) was used for ChIP-qPCR. Amplification specificity and efficiency were confirmed with melting curve analysis, slope analysis, and agarose gel electrophoresis. Primers were listed in Supple Table.

Tumorigenesis.

The efforts of all animal experiments were made to minimize suffering. The studies were carried out in strict accordance with the recommendations in the Guide for the Care and Use of Laboratory Animals of the Japanese Pharmacological Society. The protocol was approved by the Animal Care and Use Committee, Okayama University (Permit Number: OKU-2016219). All animals were held under specific pathogen-free conditions. PC-3 cells (5×10^5) were transfected with 40 pmol MZF1-targeted siRNA, 10 µg pCMV6-ScanD1-myc-Flag or 10 µg pCMV-EGFP via electroporation, cultured for 5 days, and then 2.5×10^6 cells were subcutaneously injected on a back of a 6-7-years-old SCID mouse (CLEA Japan, Tokyo). Tumor volumes were measured at day 41 post-injection period. The major axis (a) and minor axis (b) of tumors were measured with a caliper. The tumors were deemed to be ellipsoid and the volumes were calculated with a formula as follows: a tumor volume (V) $\fallingdotseq 4\pi ab^2/3$.

Western blotting.

To compare CDC37 levels among several types of cells, cells were cultured to reach confluent in a 6-cm dish or sparsely grown in a 10-cm dish. For endogenous SCAND1, protein samples were collected when cells reached sub-confluent. At day 2 after medium replacement, cells were washed with PBS and lysed within CelLytic M (Sigma, St. Louis, MO) for 15 min with

gentle shaking. Lysates were collected and centrifuged at 14,000 × *g* for 15 min. Protein concentration was measured using BCA protein assay (Thermo Fisher Scientific). Protein samples (10-40 µg: equal amount) were loaded to SDS-PAGE. Proteins were transferred to PVDF membrane with a semi-dry method. The membranes were blocked within 5% skimmed milk in TBST for 1 hour. The membranes were incubated with primary antibodies overnight at 4°C and with secondary antibodies for 1 hour at RT. The membranes were washed 3 times with TBST for 15 min after each antibody reactions. Chemiluminescence was detected with ChemiDoc MP Imaging System (Bio-Rad).

For crosslinked chromatin western blotting, see "chromatin" section. For overexpression of MZF1 and SCAND1 in PC-3, cells were transfected with pcDNA3/Flag-MZF1 or pcDNA3(-) using FuGENE6 (Roche) and cultured for 24 hours. Cells were washed with ice-cold PBS twice and lysed within RIPA buffer supplemented with protease phosphatase inhibitor cocktail (Thermo Fisher Scientific) at 4°C for 15 min, and then collected. The lysed cells were homogenized 10 times using a 25-gauge needle attached to a 1-ml syringe and then incubated on ice for 30 min. The lysate was centrifuged at 12,000 × *g* for 20 min at 4°C to remove debris. The same amount of the protein samples (10-50 µg) were used for SDS-PAGE and semi-dry transfer.

For depletion of MZF1, DU-145 cultured in 6-well plate was transfected with siRNA hMZF1-all-NM_003422-53 using Lipofectamine RNAi Max following manufacturer's instruction. The medium was replaced with a fresh one at 24 hours after the transfection. Cells were collected using trypsin and counted at 48 hours after the transfection. The cell lysate was prepared using RIPA buffer as described above. The equal amount of lysate (25 µg) was loaded to each lane for SDS-PAGE (4-20% TGX gel, BioRad). The proteins were transferred to a PVDF membrane with the wet-transfer method at 40V for 16 hours on ice

with a transfer buffer (25 mM Tris, 192 mM Glycine, 10% methanol, and 0.05% SDS). The membrane was washed 3 times with TBST for 15 min and then blocked 1 hour within 5% skimmed milk. MZF1, CDC37, HSP90α, and HSP90β were detected by western blotting.

The antibodies used were anti-MZF1 (C10502, Assay Biotechnology, 1:500), anti-CDC37 (D11A3, Cell Signaling Technology, 1:1000), anti-FLAG (Clone M2, Sigma), anti-SCAND1 (ab64828, Abcam, Cambridge, UK), and HRP-conjugated anti-GAPDH antibody (Clone 5A12, Fujifilm Wako, 1:5000).

Immunocytochemistry.

Immunocytochemistry was performed as described [59]. Cells cultured in 4-well chamber slides were fixed with 4% (wt/vol) paraformaldehyde in PBS for 15 min. Cells were permeabilized with 0.2% Triton X-100 in PBS for 15 min. Cells were blocked in IHC/ICC blocking buffer high protein (eBioscience, San Diego, CA) for 10 min and then reacted with anti-MZF1 antibody (1:50, C10502; Assay Biotechnology, Fremont, CA) and AlexaFluor488 secondary antibody (Thermo Fisher Scientific, 1:1000) in the blocking buffer. Cells were washed with PBS for 5 min twice between the steps. Cells were mounted with ProLong Gold AntiFade Reagent (Thermo Fisher Scientific). Fluorescence images were captured using Axio Vision microscope equipped with an AxioCam MR3 (Zeiss, Oberkochen, Germany).

RT-qPCR.

RT-qPCR was performed as previously described [59,60]. Total RNA was prepared using an RNeasy RNA purification system (Qiagen, Hilden, Germany) with *DNase* I treatment. cDNA was synthesized using an RT kit for qRT-PCR (Qiagen) with a mixture of oligo dT and random primers. The cDNA pool was diluted 5- to 20-fold. The cDNA standard with permissible slopes

Peer-reviewed version available at Cancers 2019, 11, 792; doi:10.3390/cancers11060792

of PCR efficiencies was prepared by step dilution of the cDNA pool for relative quantification of mRNA levels. In 20 µl of qPCR mix, 0.25 µM of each primer, 4-10 µl of diluted cDNA, and 10 µl SYBR green 2x Master Mix (Applied Biosystems, Waltham, MA) was added and reacted at 95°C for 10 min, followed by 40 cycles at 95°C for 15 seconds and 60°C for 1 min. Dissociation curves with specific single-peaked PCR and proper amplification slopes for PCR efficiency were confirmed. LinRegPCR software was used for baseline fluorescence correction, and calculation of Cq values and PCR efficiency of amplicons [61]. Primer sequences are listed in Supple Table.

Gene expression in clinical samples.

Co-expression of MZF1 and CDC37 was analyzed in TCGA in cBioPortal. Data sets of NEPC/CRPC (Trento/Cornell/Broad 2016, 114 samples) and prostate adenocarcinomas (TCGA, PanCancer Atlas; 494 patients/samples) were analyzed and Spearman's rank correlation coefficient of co-expression was shown on the figure.

For correlation of gene expression with patient prognosis, Kaplan-Meier survival analysis was performed using 494 prostate cancer patient samples in the Human Protein Atlas Database.

Statistics. Data were expressed as the means ± SD unless otherwise specified. Comparisons of 2 were done with an unpaired Student's *t*-test.

Acknowledgments: This paper is dedicated to the memory of one of our mentors, Professor Ken-ichi Kozaki, who passed away on May 29, 2016. The authors thank Barbara Wegiel, Eva Csizmadia, Ayesha Murshid, Yuka Okusha, Kuniaki Okamoto, and Yasutomo Nasu for valuable, illuminating discussion and encouragement. The authors thank Sachin Doshi for technical assistance.

Funding: This work was supported by NIH research grants: RO1CA119045, RO1CA47407, and RO1CA176326 (SKC) and by JSPS KAKENHI grants JP17K11642 (TE), JP17K11669-KOh (TE CS), and JP17K11643 (CS TE) and by Suzuken Memorial Foundation grant (TE).

Conflicts of Interest: The authors declare no conflict of interest with the content of this study.

Preprints (www.preprints.org) | NOT PEER-REVIEWED | Posted: 6 May 2019 doi:10.20944/preprints201905.0062.v1

Peer-reviewed version available at Cancers 2019, 11, 792; doi:10.3390/cancers11060792

Table 1. Correlation between gene expression and prognosis of prostate cancer patients.

	P value	N (total)	N (high)	N (low)
MZF1	**0.0287**	494	99	395
CDC37	**0.0182**	494	198	296
PSA	0.154	494	389	105

Supplemental Items

Fig S1. Binding sites for MZF1 and HSF1 in *CDC37*. MZF1 binding sites were enclosed with blue boxes. Heat shock elements (HSE) were shown with red. The sequences detected by forwarding primers (F) and reverse primers (R) in ChIP-qPCR were underlined.

Table S1. List of siRNA sequences.

Name of siRNA	Sequence (5' to 3')
hMZF1-all-NM_003422-53 sense	ccaagccuuucuccauuuuTT
hMZF1-all-NM_003422-53 antisense	aaaauggagaaaggcuuggTT

Table S2. List of primers for ChIP-qPCR.

Name of primers	Sequence (5' to 3')
CDC37/-1750F/160bp	AGGGACAGTGCAAAGCAACT
CDC37/-1750R/160bp	GCTTCAGCAAAACAGGGTTC
CDC37/-380F/115bp	TACCACCCCCGATTTAGACA
CDC37/HSE/-380R/115bp	CTTCGTAAACGGGGACCTAA

Table S3. List of primers for qRT-PCR.

CDC37-h1030F/1693	TCCAGAAGTGCTTCGATGTG
CDC37-h1140R/1693	AGAGGCCAGAGTCAATGCAG

MZF1-h785F/2620	TGCAGGTGAAAGAGGAGTCA
MZF1-h939R/2620	AGTCTTGCTGTGGGGAAAGA
RPL32 F	CAGGGTTCGTAGAAGATTCAAGGG
RPL32 R	CTTGGAAACATTGTGAGCGATC

References

1. Kimura, Y.; Rutherford, S.L.; Miyata, Y.; I., Y.; Freeman, B.C.; Yue, L.; Morimoto, R.I.; Lindquist, S. Cdc37 is a molecular chaperone with specific functions in signal transduction. *Genes & Development* **1997**, *11*, 1775-1785.
2. Silverstein, A.M.; Grammatikakis, N.; Cochran, B.H.; Chinkers, M.; Pratt, W.B. p50 cdc37 binds directly to the catalytic domain of Raf as well as to a site on hsp90 that is topologically adjacent to the tetratricopeptide repeat binding site. *J Biol Chem* **1998**, *273*, 20090-20095.
3. Basso, A.D.; Solit, D.B.; Chiosis, G.; Giri, B.; Tsichlis, P.; Rosen, N. Akt forms an intracellular complex with heat shock protein 90 (Hsp90) and Cdc37 and is destabilized by inhibitors of Hsp90 function. *J Biol Chem* **2002**, *277*, 39858-39866, doi:10.1074/jbc.M206322200.
4. Chen, G.Y.; Cao, P.; Goeddel, D.V. TNF-induced recruitment and activation of the IKK complex require Cdc37 and Hsp90. *Mol Cell* **2002**, *9*, 401-410.
5. Dai, K.; Kobayashi, R.; Beach, D. Physical interactionof mammalian CDC37 with CDK4. *J Biol Chem* **1996**, *271*, 22030-22034.
6. Stepanova, L.; Leng, X.; Parker, S.B.; Harper, J.W. Mammalian p50 Cdc37 is aprotein kinase-targeting subunit of Hsp90 that binds and stabilize Cdk4. *Genes & Development* **1996**, *10*, 1491-1502.
7. Vaughan, C.K.; Gohlke, U.; Sobott, F.; Good, V.M.; Ali, M.M.; Prodromou, C.; Robinson, C.V.; Saibil, H.R.; Pearl, L.H. Structure of an Hsp90-Cdc37-Cdk4 complex. *Mol Cell* **2006**, *23*, 697-707, doi:10.1016/j.molcel.2006.07.016.
8. Siligardi, G.; Panaretou, B.; Meyer, P.; Singh, S.; Woolfson, D.N.; Piper, P.W.; Pearl, L.H.; Prodromou, C. Regulation of Hsp90 ATPase activity by the co-chaperone Cdc37p/p50cdc37. *J Biol Chem* **2002**, *277*, 20151-20159, doi:10.1074/jbc.M201287200.
9. Roe, S.M.; Ali, M.M.U.; Meyer, P.; Vaughan, C.K.; Panaretou, B.; Piper, P.W.; Prodromou, C.; Pearl, L.H. The mechanism of Hsp90 regulation by the protein kinase-specific cochaperone p50 cdc37. *Cell* **2004**, *116*, 87-98.
10. Stepanova, L.; Yang, G.; DeMayo, F.; Wheeler, T.M.; Finegold, M.; Thompson, T.C.; Harper, J.W. Induction of human CDC37 in prostate cancer correlates with the ability of targeted CDC37 expression to promote prostatic hyperplasia. *Oncogene* **2000**, *19*, 2186-2193.
11. Gray, P.J., Jr.; Stevenson, M.A.; Calderwood, S.K. Targeting Cdc37 inhibits multiple signaling pathways and induces growth arrest in prostate cancer cells. *Cancer Res* **2007**, *67*, 11942-11950, doi:10.1158/0008-5472.CAN-07-3162.
12. Gray, P.J.; Prince, T.; Cheng, J.; Stevenson, M.A.; Calderwood, S.K. Targeting the

oncogene and kinome chaperone CDC37. *Nat Rev Cancer* **2008**, *8*, 491-495.

13. Calderwood, S.K. Cdc37 as a co-chaperone to Hsp90. *Subcell Biochem* **2015**, *78*, 103-112, doi:10.1007/978-3-319-11731-7_5.
14. Smith, J.R.; de Billy, E.; Hobbs, S.; Powers, M.; Prodromou, C.; Pearl, L.; Clarke, P.A.; Workman, P. Restricting direct interaction of CDC37 with HSP90 does not compromise chaperoning of client proteins. *Oncogene* **2015**, *34*, 15-26, doi:10.1038/onc.2013.519.
15. Neckers, L.; Workman, P. Hsp90 molecular chaperone inhibitors: are we there yet? *Clin Cancer Res* **2012**, *18*, 64-76, doi:10.1158/1078-0432.CCR-11-1000.
16. Huang, L.; Grammatikakis, N.; Toole, B.P. Organization of the Chick CDC37 Gene. *J Biol Chem* **1998**, *273*, 3598-3603.
17. Eguchi, T.; Prince, T.; Wegiel, B.; Calderwood, S.K. Role and Regulation of Myeloid Zinc Finger Protein 1 in Cancer. *J Cell Biochem* **2015**, *116*, 2146-2154, doi:10.1002/jcb.25203.
18. Perrotti, D.; Melotti, P.; Skorski, T.; Casella, I.; Peschle, C.; Calabretta, B. Overexpression of the zinc finger protein MZF1 inhibits hematopoietic development from embryonic stem cells: correlation with negative regulation of CD34 and c-myb promoter activity. *Mol Cell Biol* **1995**, *15*, 6075-6087.
19. Rafn, B.; Nielsen, C.F.; Andersen, S.H.; Szyniarowski, P.; Corcelle-Termeau, E.; Valo, E.; Fehrenbacher, N.; Olsen, C.J.; Daugaard, M.; Egebjerg, C., et al. ErbB2-driven breast cancer cell invasion depends on a complex signaling network activating myeloid zinc finger-1-dependent cathepsin B expression. *Mol Cell* **2012**, *45*, 764-776, doi:10.1016/j.molcel.2012.01.029.
20. Weber, C.E.; Kothari, A.N.; Wai, P.Y.; Li, N.Y.; Driver, J.; Zapf, M.A.; Franzen, C.A.; Gupta, G.N.; Osipo, C.; Zlobin, A., et al. Osteopontin mediates an MZF1-TGF-beta1-dependent transformation of mesenchymal stem cells into cancer-associated fibroblasts in breast cancer. *Oncogene* **2015**, *34*, 4821-4833, doi:10.1038/onc.2014.410.
21. Tsai, L.H.; Wu, J.Y.; Cheng, Y.W.; Chen, C.Y.; Sheu, G.T.; Wu, T.C.; Lee, H. The MZF1/c-MYC axis mediates lung adenocarcinoma progression caused by wild-type lkb1 loss. *Oncogene* **2015**, *34*, 1641-1649, doi:10.1038/onc.2014.118.
22. Hsieh, Y.H.; Wu, T.T.; Huang, C.Y.; Hsieh, Y.S.; Liu, J.Y. Suppression of tumorigenicity of human hepatocellular carcinoma cells by antisense oligonucleotide MZF-1. *Chin J Physiol* **2007**, *50*, 9-15.
23. Ko, C.P.; Yang, L.C.; Chen, C.J.; Yeh, K.T.; Lin, S.H.; Yang, S.F.; Chen, M.K.; Lin, C.W. Expression of myeloid zinc finger 1 and the correlation to clinical aspects of oral squamous cell carcinoma. *Tumour Biol* **2015**, *36*, 7099-7105, doi:10.1007/s13277-015-3419-x.
24. Lee, Y.K.; Park, U.H.; Kim, E.J.; Hwang, J.T.; Jeong, J.C.; Um, S.J. Tumor antigen PRAME is up-regulated by MZF1 in cooperation with DNA hypomethylation in melanoma cells.

Cancer Lett **2017**, *403*, 144-151, doi:10.1016/j.canlet.2017.06.015.

25. Jia, N.; Wang, J.; Li, Q.; Tao, X.; Chang, K.; Hua, K.; Yu, Y.; Wong, K.K.; Feng, W. DNA methylation promotes paired box 2 expression via myeloid zinc finger 1 in endometrial cancer. *Oncotarget* **2016**, *7*, 84785-84797, doi:10.18632/oncotarget.12626.
26. Mudduluru, G.; Vajkoczy, P.; Allgayer, H. Myeloid zinc finger 1 induces migration, invasion, and in vivo metastasis through Axl gene expression in solid cancer. *Mol Cancer Res* **2010**, *8*, 159-169, doi:10.1158/1541-7786.Mcr-09-0326.
27. Edelstein, L.C.; Collins, T. The SCAN domain family of zinc finger transcription factors. *Gene* **2005**, *359*, 1-17, doi:10.1016/j.gene.2005.06.022.
28. Williams, A.J.; Blacklow, S.C.; Collins, T. The zinc finger-associated SCAN box is a conserved oligomerization domain. *Mol Cell Biol* **1999**, *19*, 8526-8535.
29. Schumacher, C.; Wang, H.; Honer, C.; Ding, W.; Koehn, J.; Lawrence, Q.; Coulis, C.M.; Wang, L.L.; Ballinger, D.; Bowen, B.R., et al. The SCAN domain mediates selective oligomerization. *J Biol Chem* **2000**, *275*, 17173-17179, doi:10.1074/jbc.M000119200.
30. Sander, T.L.; Haas, A.L.; Peterson, M.J.; Morris, J.F. Identification of a novel SCAN box-related protein that interacts with MZF1B. The leucine-rich SCAN box mediates hetero- and homoprotein associations. *J Biol Chem* **2000**, *275*, 12857-12867.
31. Ko, H.; Kim, S.; Yang, K.; Kim, K. Phosphorylation-dependent stabilization of MZF1 upregulates N-cadherin expression during protein kinase CK2-mediated epithelial-mesenchymal transition. *Oncogenesis* **2018**, *7*, 27, doi:10.1038/s41389-018-0035-9.
32. Verma, N.K.; Gadi, A.; Maurizi, G.; Roy, U.B.; Mansukhani, A.; Basilico, C. Myeloid Zinc Finger 1 and GA Binding Protein Co-Operate with Sox2 in Regulating the Expression of Yes-Associated Protein 1 in Cancer Cells. *Stem Cells* **2017**, *35*, 2340-2350, doi:10.1002/stem.2705.
33. Luan, H.; Mohapatra, B.; Bielecki, T.A.; Mushtaq, I.; Mirza, S.; Jennings, T.A.; Clubb, R.J.; An, W.; Ahmed, D.; El-Ansari, R., et al. Loss of the Nuclear Pool of Ubiquitin Ligase CHIP/STUB1 in Breast Cancer Unleashes the MZF1-Cathepsin Pro-oncogenic Program. *Cancer Res* **2018**, *78*, 2524-2535, doi:10.1158/0008-5472.Can-16-2140.
34. Zheng, L.; Jiao, W.; Mei, H.; Song, H.; Li, D.; Xiang, X.; Chen, Y.; Yang, F.; Li, H.; Huang, K., et al. miRNA-337-3p inhibits gastric cancer progression through repressing myeloid zinc finger 1-facilitated expression of matrix metalloproteinase 14. *Oncotarget* **2016**, *7*, 40314-40328, doi:10.18632/oncotarget.9739.
35. Chen, P.M.; Cheng, Y.W.; Wang, Y.C.; Wu, T.C.; Chen, C.Y.; Lee, H. Up-regulation of FOXM1 by E6 oncoprotein through the MZF1/NKX2-1 axis is required for human papillomavirus-associated tumorigenesis. *Neoplasia* **2014**, *16*, 961-971, doi:10.1016/j.neo.2014.09.010.

36. Wu, L.; Han, L.; Zhou, C.; Wei, W.; Chen, X.; Yi, H.; Wu, X.; Bai, X.; Guo, S.; Yu, Y., et al. TGF-beta1-induced CK17 enhances cancer stem cell-like properties rather than EMT in promoting cervical cancer metastasis via the ERK1/2-MZF1 signaling pathway. *Febs j* **2017**, *284*, 3000-3017, doi:10.1111/febs.14162.

37. Horinaka, M.; Yoshida, T.; Tomosugi, M.; Yasuda, S.; Sowa, Y.; Sakai, T. Myeloid zinc finger 1 mediates sulindac sulfide-induced upregulation of death receptor 5 of human colon cancer cells. *Sci Rep* **2014**, *4*, 6000, doi:10.1038/srep06000.

38. Lee, E.H.; Ji, K.Y.; Kim, E.M.; Kim, S.M.; Song, H.W.; Choi, H.R.; Chung, B.Y.; Choi, H.J.; Bai, H.W.; Kang, H.S. Blockade of Axl signaling ameliorates HPV16E6-mediated tumorigenecity of cervical cancer. *Sci Rep* **2017**, *7*, 5759, doi:10.1038/s41598-017-05977-8.

39. Lee, C.J.; Hsu, L.S.; Yue, C.H.; Lin, H.; Chiu, Y.W.; Lin, Y.Y.; Huang, C.Y.; Hung, M.C.; Liu, J.Y. MZF-1/Elk-1 interaction domain as therapeutic target for protein kinase Calpha-based triple-negative breast cancer cells. *Oncotarget* **2016**, *7*, 59845-59859, doi:10.18632/oncotarget.11337.

40. Yue, C.H.; Huang, C.Y.; Tsai, J.H.; Hsu, C.W.; Hsieh, Y.H.; Lin, H.; Liu, J.Y. MZF-1/Elk-1 Complex Binds to Protein Kinase Calpha Promoter and Is Involved in Hepatocellular Carcinoma. *PLoS One* **2015**, *10*, e0127420, doi:10.1371/journal.pone.0127420.

41. Chen, Y.; Zhang, Z.; Yang, K.; Du, J.; Xu, Y.; Liu, S. Myeloid zinc-finger 1 (MZF-1) suppresses prostate tumor growth through enforcing ferroportin-conducted iron egress. *Oncogene* **2015**, *34*, 3839-3847, doi:10.1038/onc.2014.310.

42. Lin, S.; Wang, X.; Pan, Y.; Tian, R.; Lin, B.; Jiang, G.S.; Chen, K.; He, Y.Q.; Zhang, L.; Zhai, W., et al. Transcription Factor Myeloid Zinc-Finger 1 Suppresses Human Gastric Carcinogenesis by Interacting with Metallothionein 2A. *Clin Cancer Res* **2019**, doi:10.1158/1078-0432.CCR-18-1281.

43. Lee, J.H.; Kim, S.S.; Lee, H.S.; Hong, S.; Rajasekaran, N.; Wang, L.H.; Choi, J.S.; Shin, Y.K. Upregulation of SMAD4 by MZF1 inhibits migration of human gastric cancer cells. *Int J Oncol* **2017**, *50*, 272-282, doi:10.3892/ijo.2016.3793.

44. Tsai, S.J.; Hwang, J.M.; Hsieh, S.C.; Ying, T.H.; Hsieh, Y.H. Overexpression of myeloid zinc finger 1 suppresses matrix metalloproteinase-2 expression and reduces invasiveness of SiHa human cervical cancer cells. *Biochem Biophys Res Commun* **2012**, *425*, 462-467, doi:10.1016/j.bbrc.2012.07.125.

45. Vishwamitra, D.; Curry, C.V.; Alkan, S.; Song, Y.H.; Gallick, G.E.; Kaseb, A.O.; Shi, P.; Amin, H.M. The transcription factors Ik-1 and MZF1 downregulate IGF-IR expression in NPM-ALK(+) T-cell lymphoma. *Mol Cancer* **2015**, *14*, 53, doi:10.1186/s12943-015-0324-2.

46. Ogawa, H.; Ueda, T.; Aoyama, T.; Aronheim, A.; Nagata, S.; Fukunaga, R. A SWI2/SNF2-type ATPase/helicase protein, mDomino, interacts with myeloid zinc finger protein 2A (MZF-2A) to regulate its transcriptional activity. *Genes Cells* **2003**, *8*, 325-339.

47. Brix, D.M.; Tvingsholm, S.A.; Hansen, M.B.; Clemmensen, K.B.; Ohman, T.; Siino, V.; Lambrughi, M.; Hansen, K.; Puustinen, P.; Gromova, I., et al. Release of transcriptional repression via ErbB2-induced, SUMO-directed phosphorylation of myeloid zinc finger-1 serine 27 activates lysosome redistribution and invasion. *Oncogene* **2019**, *38*, 3170-3184, doi:10.1038/s41388-018-0653-x.

48. Workman, P.; Burrows, F.; Neckers, L.; Rosen, N. Drugging the cancer chaperone HSP90: combinatorial therapeutic exploitation of oncogene addiction and tumor stress. *Ann N Y Acad Sci* **2007**, *1113*, 202-216, doi:10.1196/annals.1391.012.

49. Eguchi, T.; Sogawa, C.; Okusha, Y.; Uchibe, K.; Iinuma, R.; Ono, K.; Nakano, K.; Murakami, J.; Itoh, M.; Arai, K., et al. Organoids with cancer stem cell-like properties secrete exosomes and HSP90 in a 3D nanoenvironment. *PLoS One* **2018**, *13*, e0191109, doi:10.1371/journal.pone.0191109.

50. Ono, K.; Eguchi, T.; Sogawa, C.; Calderwood, S.K.; Futagawa, J.; Kasai, T.; Seno, M.; Okamoto, K.; Sasaki, A.; Kozaki, K.I. HSP-enriched properties of extracellular vesicles involve survival of metastatic oral cancer cells. *J Cell Biochem* **2018**, *119*, 7363-7376, doi:10.1002/jcb.27039.

51. Nolan, K.D.; Kaur, J.; Isaacs, J.S. Secreted heat shock protein 90 promotes prostate cancer stem cell heterogeneity. *Oncotarget* **2017**, *8*, 19323-19341, doi:10.18632/oncotarget.14252.

52. de la Mare, J.A.; Jurgens, T.; Edkins, A.L. Extracellular Hsp90 and TGFbeta regulate adhesion, migration and anchorage independent growth in a paired colon cancer cell line model. *BMC Cancer* **2017**, *17*, 202, doi:10.1186/s12885-017-3190-z.

53. Dong, H.; Zou, M.; Bhatia, A.; Jayaprakash, P.; Hofman, F.; Ying, Q.; Chen, M.; Woodley, D.T.; Li, W. Breast Cancer MDA-MB-231 Cells Use Secreted Heat Shock Protein-90alpha (Hsp90alpha) to Survive a Hostile Hypoxic Environment. *Sci Rep* **2016**, *6*, 20605, doi:10.1038/srep20605.

54. Dreos, R.; Ambrosini, G.; Groux, R.; Cavin Perier, R.; Bucher, P. The eukaryotic promoter database in its 30th year: focus on non-vertebrate organisms. *Nucleic Acids Res* **2017**, *45*, D51-d55, doi:10.1093/nar/gkw1069.

55. Messeguer, X.; Escudero, R.; Farre, D.; Nunez, O.; Martinez, J.; Alba, M.M. PROMO: detection of known transcription regulatory elements using species-tailored searches. *Bioinformatics* **2002**, *18*, 333-334.

56. Eguchi, T.; Kubota, S.; Takigawa, M. Promoter Analyses of CCN Genes. *Methods Mol Biol* **2017**, *1489*, 177-185, doi:10.1007/978-1-4939-6430-7_18.

57. Eguchi, T.; Calderwood, S.K.; Takigawa, M.; Kubota, S.; Kozaki, K.I. Intracellular MMP3 Promotes HSP Gene Expression in Collaboration With Chromobox Proteins. *J Cell Biochem* **2017**, *118*, 43-51, doi:10.1002/jcb.25607.

58. Namba, Y.; Sogawa, C.; Okusha, Y.; Kawai, H.; Itagaki, M.; Ono, K.; Murakami, J.; Aoyama, E.; Ohyama, K.; Asaumi, J.I., et al. Depletion of Lipid Efflux Pump ABCG1 Triggers the Intracellular Accumulation of Extracellular Vesicles and Reduces Aggregation and Tumorigenesis of Metastatic Cancer Cells. *Front Oncol* **2018**, *8*, 376, doi:10.3389/fonc.2018.00376.

59. Eguchi, T.; Kubota, S.; Kawata, K.; Mukudai, Y.; Uehara, J.; Ohgawara, T.; Ibaragi, S.; Sasaki, A.; Kuboki, T.; Takigawa, M. Novel transcription-factor-like function of human matrix metalloproteinase 3 regulating the CTGF/CCN2 gene. *Mol Cell Biol* **2008**, *28*, 2391-2413, doi:10.1128/MCB.01288-07.

60. Eguchi, T.; Watanabe, K.; Hara, E.S.; Ono, M.; Kuboki, T.; Calderwood, S.K. OstemiR: a novel panel of microRNA biomarkers in osteoblastic and osteocytic differentiation from mesencymal stem cells. *PLoS One* **2013**, *8*, e58796, doi:10.1371/journal.pone.0058796.

61. Ruijter, J.M.; Ramakers, C.; Hoogaars, W.M.; Karlen, Y.; Bakker, O.; van den Hoff, M.J.; Moorman, A.F. Amplification efficiency: linking baseline and bias in the analysis of quantitative PCR data. *Nucleic Acids Res* **2009**, *37*, e45, doi:10.1093/nar/gkp045.

Peer-reviewed version available at Cancers 2019, 11, 792; doi:10.3390/cancers11060792

Figure Legends

Fig 1. Elevated expression of CDC37 is caused by MZF1 in prostate cancer.

(A) Western blot showing CDC37 in prostate cancer cells. Cell lysates were prepared from confluent (Conf) and growing (Gro) RWPE-1, LNCaP, PC-3, and DU-145 cells. (B) Immunocytochemistry showing MZF1 expression and localization in PC-3 and PNT2 cells. Arrows indicate nuclear bodies of MZF1 (MZF1-NBs) seen in PC-3 but not in PNT2. (C) The number of MZF1-NBs per cells. (D) Western blot showing CDC37 altered by overexpressed MZF1 in DU-145. (E) Western blot showing CDC37 altered by depletion of MZF1 in DU-145 cells. (F) mRNA levels of CDC37 and MZF1 altered by depletion of MZF1. The MZF1-targeting siRNA mixture (A+B+C, 10 nM each) or a non-silencing control (si-ctrl) was transfected into PC-3 cells. RPL32, internal control. R-ctrl, reagent only control. *$p < 0.05$, $n = 3$. Similar results were obtained from 3 independent experiments. (G) Co-expression of MZF1 and CDC37 in patient samples of castration resistant prostate cancer (CRPC). N=114, Spearman correlation score 0.78, P=2.60e-11. (H) Co-expression of MZF1 and CDC37 in patient samples of prostate adenocarcinoma (Pr. Adeno). N=494, Spearman correlation score 0.57, P=7.74e-44.

Fig 2. SCAN zinc finger MZF1 directly trans-activates *CDC37* gene.

(A) Schemes of the *CDC37* promoter-reporter constructs. Truncated mutants of CDC37 promoter were connected with luciferase (*Luc*) gene. Blue box, MZF1 binding site. Orange box, heat shock element (HSE). 5'UTR, 5' untranslated region. (B) The secondary structures of native MZF1 and the SCANless (zinc-finger domain alone). S, SCAN box. Z, zinc-finger motif. DE, aspartic acid- and glutamic acid-rich region. GP, glycine- and a proline-rich region. MZF1 was overexpressed with an N-terminal Flag-tag. The SCANless was overexpressed with a C-terminal V5-tag. (C) Luciferase activities from the truncated CDC37 promoters controlled by

MZF1 and SCANless. Plasmid constructs shown in panels A and B were co-transfected into DU-145 cells. Vec., empty vector control. n=3, *P<0.05, **P<0.01 (vs Vec.). (D) Chromatin western blotting of MZF1 overexpressed in DU-145. Crosslinked chromatin was prepared from DU-145 overexpressed with MZF1. (E) ChIP-qPCR analysis showing MZF1 occupancy of *CDC37*. Chromatin was prepared from DU-145 overexpressed with Flag-MZF1 or GFP (control) and immunoprecipitated using anti-Flag antibody beads or control IgG. Co-immunoprecipitated DNA was analyzed by qPCR for *CDC37* (-1.8k or -0.4k regions) or control regions in *GAPDH* or *ACTB*. N=3, **P<0.01 (vs IgG control). Similar results were obtained from 3 independent experiments.

Fig 3. Zinc-fingerless SCAND1 suppresses *CDC37* gene and tumorigenesis of prostate cancer. (A) Western blot showing SCAND1 levels in normal prostate cells, PC-3, DU-145, and PNT2. (B) Western blot showing CDC37 lowered by SCAND1 overexpression. (C) Schemes of overexprssion constructs. (D) Schemes of truncated CDC37 promoters fused with luciferase reporter gene. (E) Luciferase activities from the truncated CDC37 promoters controlled by SCAND1 and truncated mutants of MZF1. Plasmid constructs shown in panels C and D were co-transfected into PC-3 cells. Vec., empty vector control. n=3, *P<0.05 (vs Vec.). (F) Chromatin western blot showing SCAND1 overexpressed in DU-145. Crosslinked chromatin was prepared from DU-145 overexpressed with SCAND1. (G) ChIP-qPCR analysis showing SCAND1 occupancy of CDC37. Chromatin was prepared from DU-145 overexpressed with SCAND1, MZF1, SCAN, SCAN+L or GFP (control) and immunoprecipitated using anti-Flag antibody beads. Co-immunoprecipitated DNA was analyzed by qPCR for CDC37 (-1.8k or -0.4k regions). N=3, **P<0.01 (vs IgG control). For figure 3 A-G, similar data were obatained from 3 independent experiments. (H) Tumorigenicity of PC-3 cells lowered by SCAND1 and

depletion of MZF1. SCAND1-overexpression plasmid, MZF1-targeted siRNA, and control GFP plasmid were transfected into PC-3 cells which were then xenografted to SCID mice subcutaneously.

Fig 4. Graphical abstract: positive and negative regulation of the CDC37 gene by MZF1 and SCAND1 respectively, in prostate cancer. CDC37 is a key protein that stabilizes HSP90 client kinases essential for cancer progression. Elevated expression of CDC37 in prostate cancer is caused by MZF1 transcriptional activation whereas SCAND1 negatively regulates the CDC37 gene and prostate cancer tumorigenesis. CL, client. 37, CDC37. 90, HSP90.

Preprints (www.preprints.org) | NOT PEER-REVIEWED | Posted: 6 May 2019 doi:10.20944/preprints201905.0062.v1

Peer-reviewed version available at *Cancers* **2019**, *11*, 792; doi:10.3390/cancers11060792

Fig 1

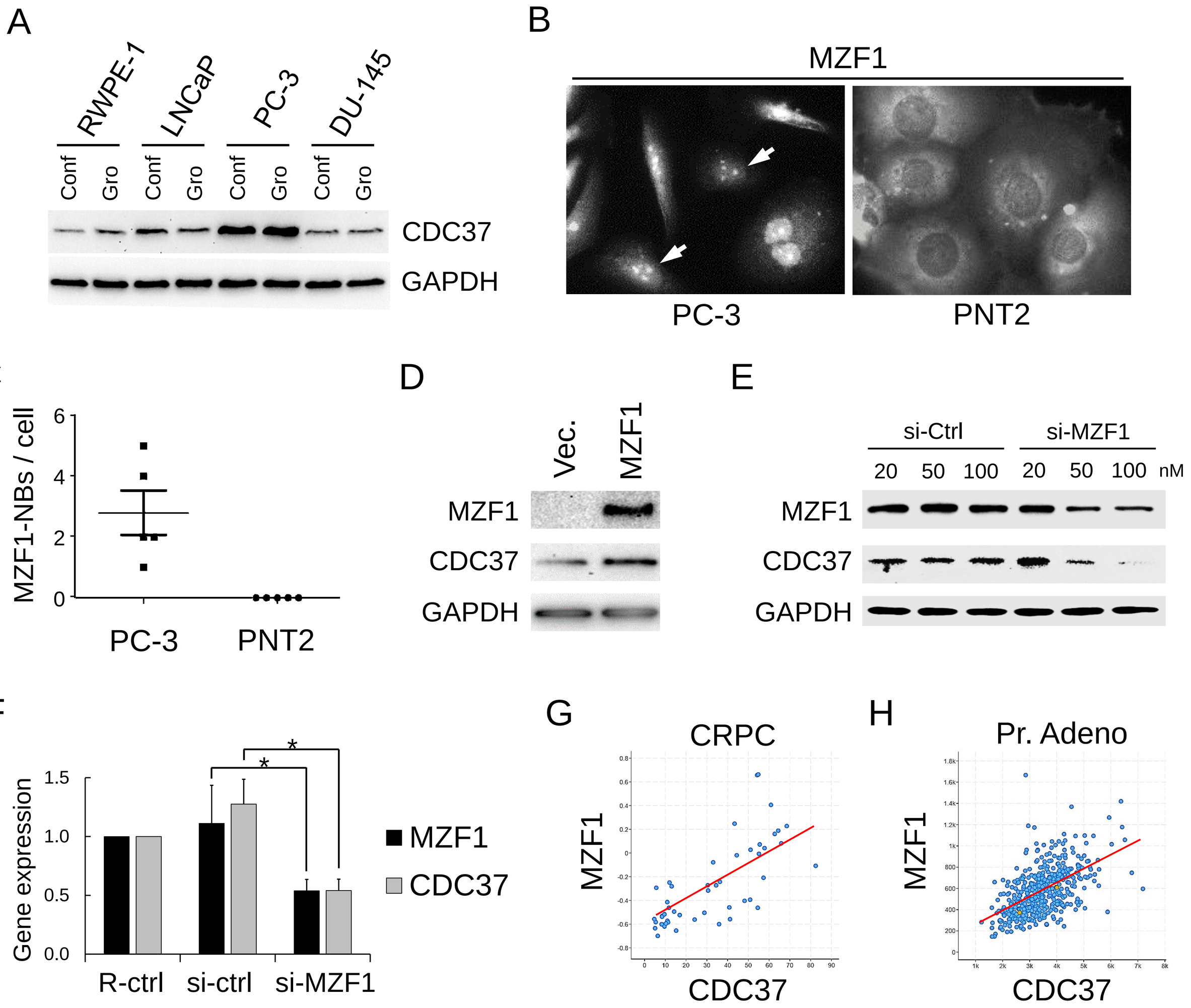

Fig 1. Elevated expression of CDC37 is caused by MZF1 in prostate cancer.

(A) Western blot showing CDC37 in prostate cancer cells. Cell lysates were prepared from confluent (Conf) and growing (Gro) RWPE-1, LNCaP, PC-3, and DU-145 cells. (B) Immunocytochemistry showing MZF1 expression and localization in PC-3 and PNT2 cells. Arrows indicate nuclear bodies of MZF1 (MZF1-NBs) seen in PC-3 but not in PNT2. (C) The number of MZF1-NBs per cells. (D) Western blot showing CDC37 altered by overexpressed MZF1 in DU-145. (E) Western blot showing CDC37 altered by depletion of MZF1 in DU-145 cells. (F) mRNA levels of CDC37 and MZF1 altered by depletion of MZF1. The MZF1-targeting siRNA mixture (A+B+C, 10 nM each) or a non-silencing control (si-ctrl) was transfected into PC-3 cells. RPL32, internal control. R-ctrl, reagent only control. *$p < 0.05$, $n = 3$. Similar results were obtained from 3 independent experiments. (G) Co-expression of MZF1 and CDC37 in patient samples of castration resistant prostate cancer (CRPC). N=114, Spearman correlation score 0.78, P=2.60e-11. (H) Co-expression of MZF1 and CDC37 in patient samples of prostate adenocarcinoma (Pr. Adeno). N=494, Spearman correlation score 0.57, P=7.74e-44.

Fig 2

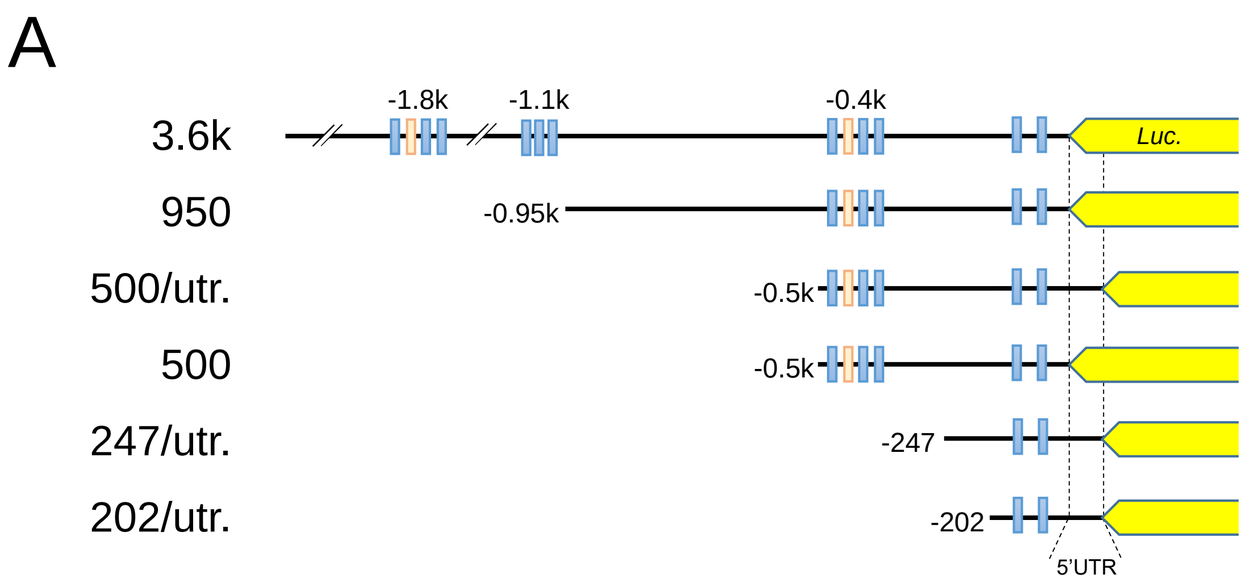

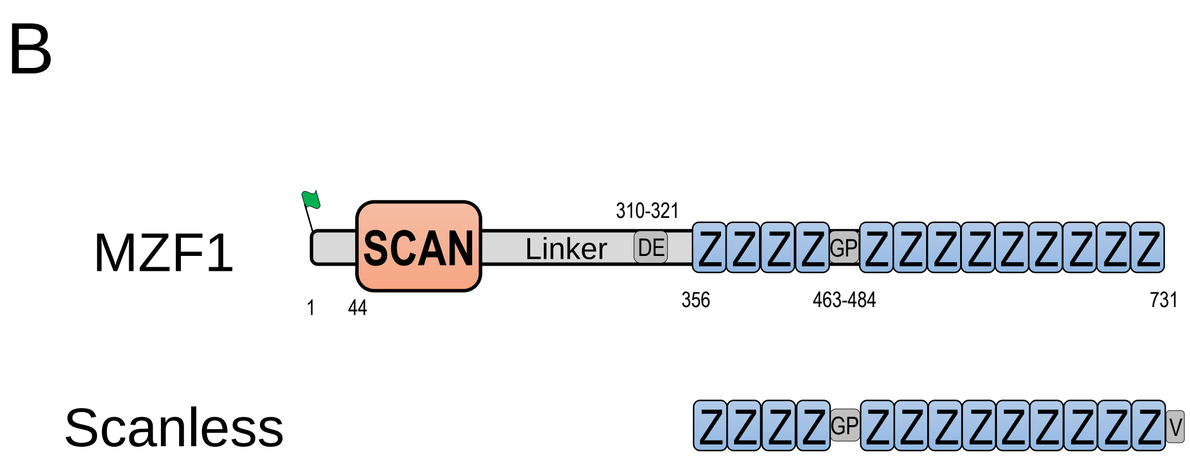

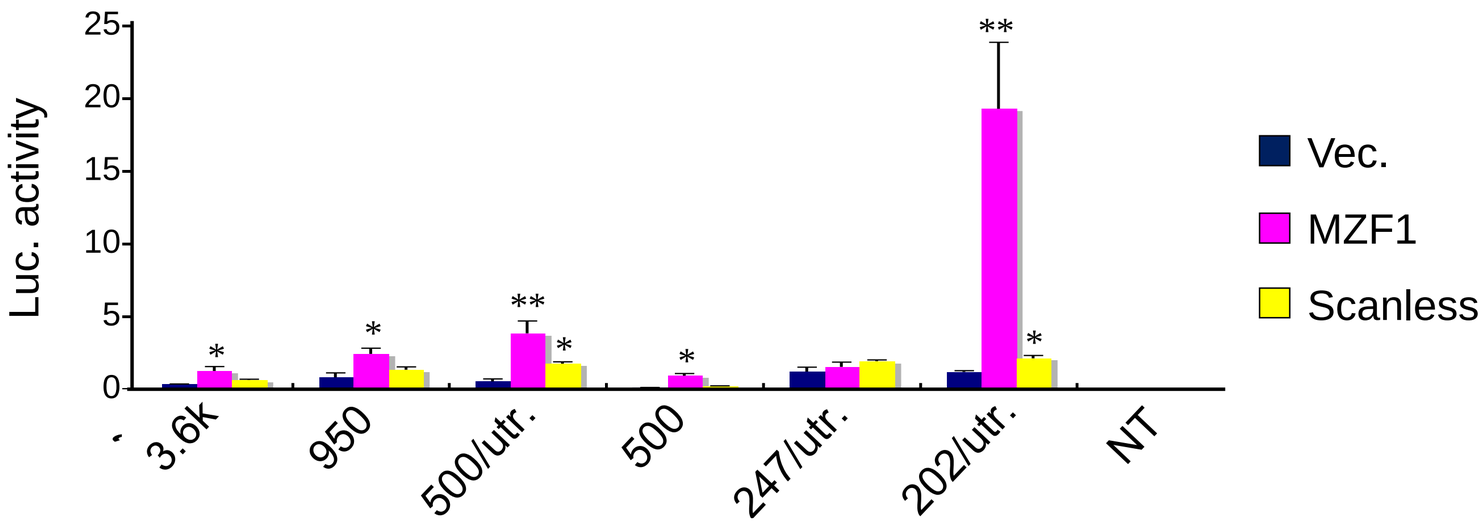

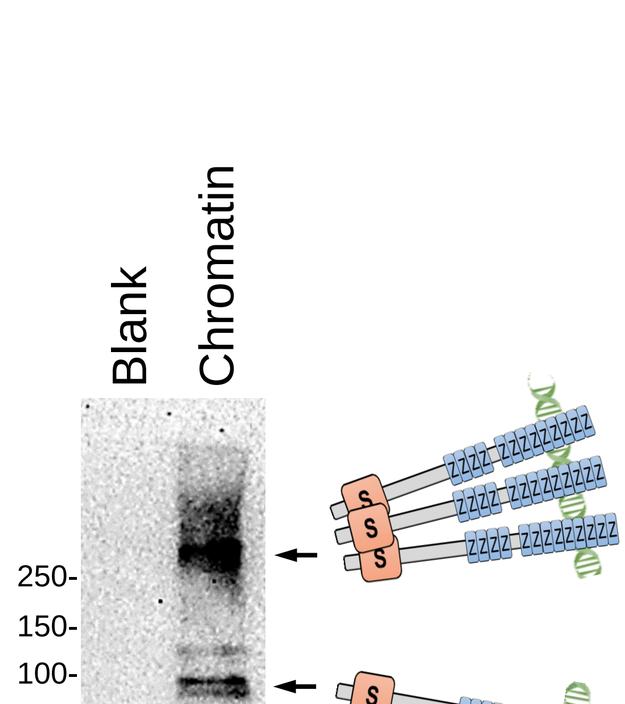

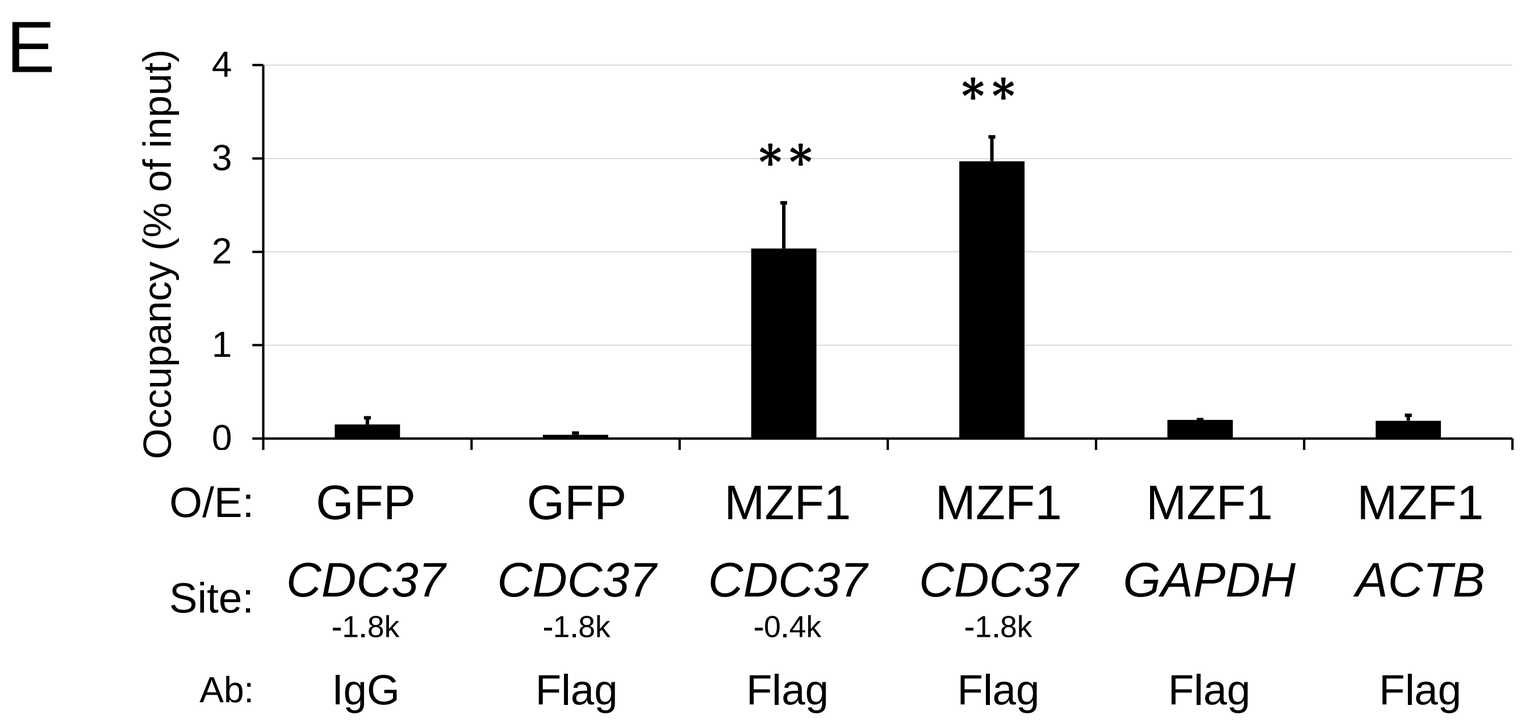

Fig 2. SCAN zinc finger MZF1 directly trans-activates *CDC37* gene.

(A) Schemes of the *CDC37* promoter-reporter constructs. Truncated mutants of CDC37 promoter were connected with luciferase (*Luc*) gene. Blue box, MZF1 binding site. Orange box, heat shock element (HSE). 5'UTR, 5' untranslated region. (B) The secondary structures of native MZF1 and the SCANless (zinc-finger domain alone). S, SCAN box. Z, zinc-finger motif. DE, aspartic acid- and glutamic acid-rich region. GP, glycine- and a proline-rich region. MZF1 was overexpressed with an N-terminal Flag-tag. The SCANless was overexpressed with a C-terminal V5-tag. (C) Luciferase activities from the truncated CDC37 promoters controlled by MZF1 and SCANless. Plasmid constructs shown in panels A and B were co-transfected into DU-145 cells. Vec., empty vector control. n=3, *P<0.05, **P<0.01 (vs Vec.). (D) Chromatin western blotting of MZF1 overexpressed in DU-145. Crosslinked chromatin was prepared from DU-145 overexpressed with MZF1. (E) ChIP-qPCR analysis showing MZF1 occupancy of *CDC37*. Chromatin was prepared from DU-145 overexpressed with Flag-MZF1 or GFP (control) and immunoprecipitated using anti-Flag antibody beads or control IgG. Co-immunoprecipitated DNA was analyzed by qPCR for *CDC37* (-1.8k or -0.4k regions) or control regions in *GAPDH* or *ACTB*. N=3, **P<0.01 (vs IgG control). Similar results were obtained from 3 independent experiments.

Fig 3

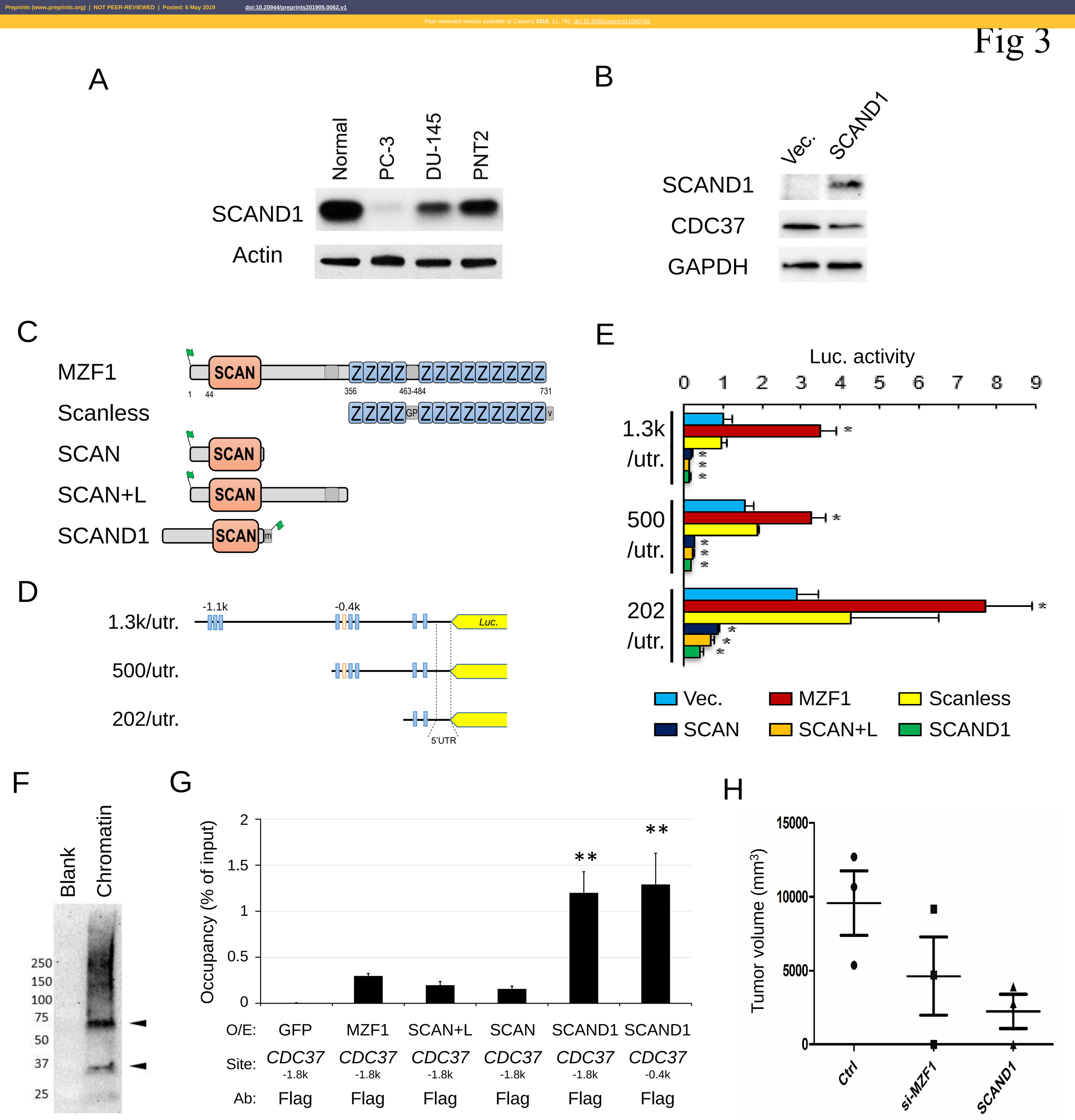

Fig 3. Zinc-fingerless SCAND1 suppresses *CDC37* gene and tumorigenesis of prostate cancer. (A) Western blot showing SCAND1 levels in normal prostate cells, PC-3, DU-145, and PNT2. (B) Western blot showing CDC37 lowered by SCAND1 overexpression. (C) Schemes of overexprssion constructs. (D) Schemes of truncated CDC37 promoters fused with luciferase reporter gene. (E) Luciferase activities from the truncated CDC37 promoters controlled by SCAND1 and truncated mutants of MZF1. Plasmid constructs shown in panels C and D were co-transfected into PC-3 cells. Vec., empty vector control. n=3, *P<0.05 (vs Vec.). (F) Chromatin western blot showing SCAND1 overexpressed in DU-145. Crosslinked chromatin was prepared from DU-145 overexpressed with SCAND1. (G) ChIP-qPCR analysis showing SCAND1 occupancy of CDC37. Chromatin was prepared from DU-145 overexpressed with SCAND1, MZF1, SCAN, SCAN+L or GFP (control) and immunoprecipitated using anti-Flag antibody beads. Co-immunoprecipitated DNA was analyzed by qPCR for CDC37 (-1.8k or -0.4k regions). N=3, **P<0.01 (vs IgG control). For figure 3 A-G, similar data were obatained from 3 independent experiments. (H) Tumorigenicity of PC-3 cells lowered by SCAND1 and depletion of MZF1. SCAND1-overexpression plasmid, MZF1-targeted siRNA, and control GFP plasmid were transfected into PC-3 cells which were then xenografted to SCID mice subcutaneously.

Preprints (www.preprints.org) | NOT PEER-REVIEWED | Posted: 6 May 2019 doi:10.20944/preprints201905.0062.v1

Peer-reviewed version available at *Cancers* **2019**, *11*, 792; doi:10.3390/cancers11060792

Fig 4

A

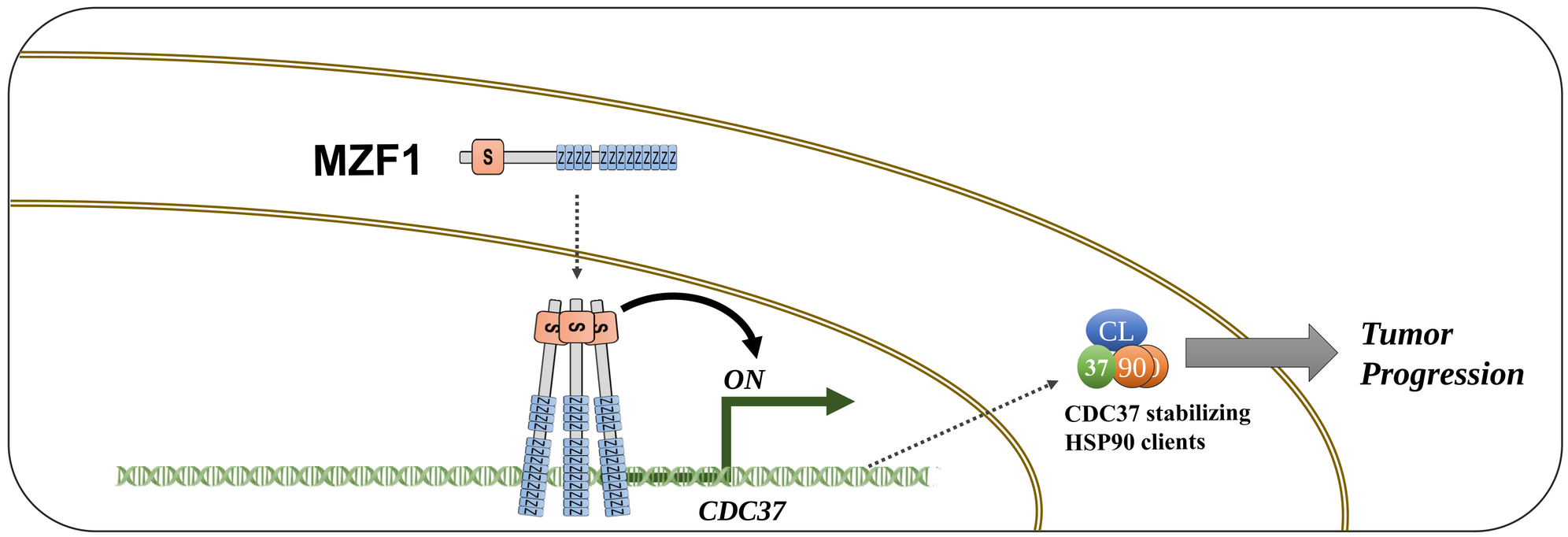

B

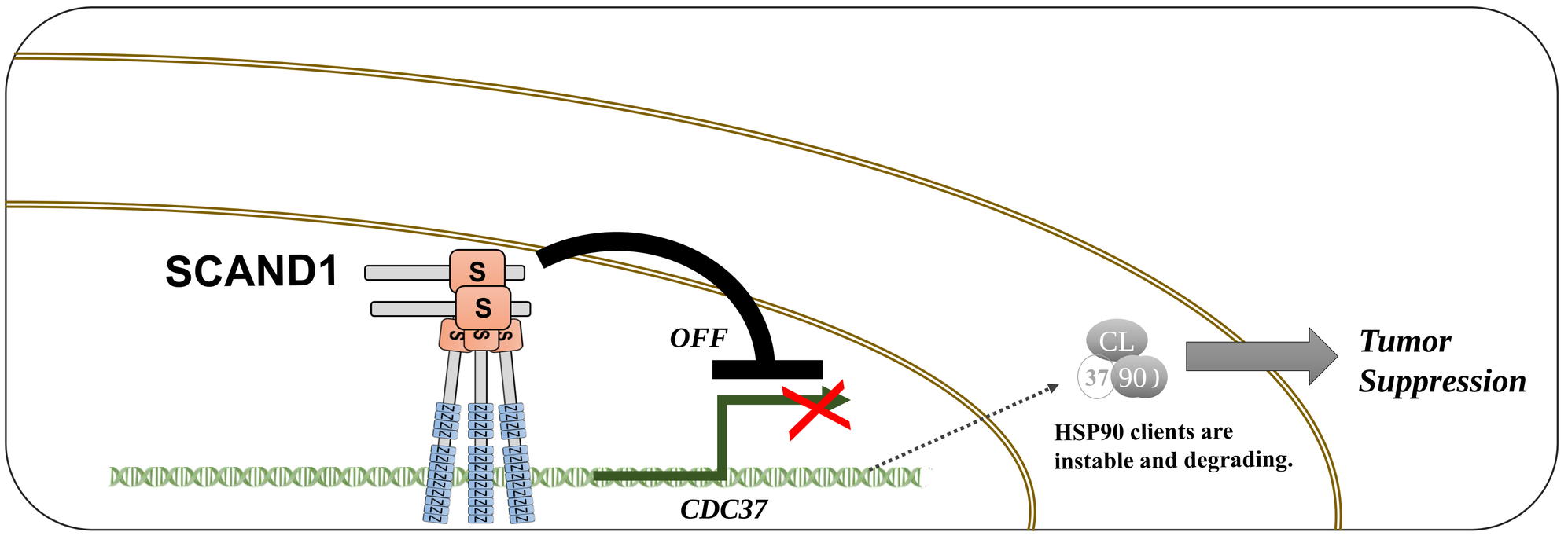

Fig 4. Graphical abstract: positive and negative regulation of the CDC37 gene by MZF1 and SCAND1 respectively, in prostate cancer. CDC37 is a key protein that stabilizes HSP90 client kinases essential for cancer progression. Elevated expression of CDC37 in prostate cancer is caused by MZF1 transcriptional activation whereas SCAND1 negatively regulates the CDC37 gene and prostate cancer tumorigenesis. CL, client. 37, CDC37. 90, HSP90.

Preprints (www.preprints.org) | NOT PEER-REVIEWED | Posted: 6 May 2019 doi:10.20944/preprints201905.0062.v1

Peer-reviewed version available at *Cancers* **2019**, *11*, 792; doi:10.3390/cancers11060792

Fig S1

CDC37/-1750

```
-1900 TAGCAGGGTTTGCACCGATG GGGGTGGGATGGGGACCGGG GACAGAGGGACAGTGCAAAG CAACTTAGGGGTCTCTCTCC TCAGTCCCCAGGGCTGGAGG
                                                                    F
-1800 TGCTGTGCTGGCAGATTAGG AAATGCTTGGGGTTGATGGG GAAGCTTCCGGCGCTCTATC CCCAGTTCTGGAAGCTGAGG CTCCGGGGAACCCTGTTTTGC
                          HSE-C            MZF    HSE                      MZF                              R
-1700 TGAAGCTGGGCAGCTCCAGT CTCCAGAGCCAGGAAGAGAC CCCCGCGCCTATCCGGGAAT CCCCGACATCTGGGATTCTC TCCAAACACCCCCAGGCTGA
```

CDC37/-1110

```
-1300 CCGGGCCGTGACGGCCACTG ATGTGCTGGACTGCCAGGGT GGAGGGGAAGAGGGAGGGGT AGGAGATGGGGACTCCCCCG CCCCTGCCCGCCCACTCGCG
-1200 GGTTTGAATGAAGCGCGAGG GGGAAGGGCGGCAGCGGGAG GACGTTTTTGTCCGATGGCC CTTCCCGCTCCATGCACCGG GGAATCCTCCCCCTTCTGGA
                      MZF                              F                                MZF   HSE
-1100 GAACTTCGCTCGCTCTCTCC AGGCACTGCCTCCAACGTCG GCTCCAGGGGAGACTAGGAA GAGGCGCCCCTCACCGGAGT GGCTGGAGCTCCTCCTATCC
         R
```

CDC37/-380

```
-500 CCCCAGCTCCCAAGGCAGGG CCACAGTCTCCCCTCCACGT TTAACCCTGCAAGGGGAGGG CCATACCACCCCCGATTTAG ACACCCCCAGGGCAGGTCCA
                                                                                  F
-400 GTCCTCCTCGGGCTGAGAAA GTCCGAGGAGTCATCAGGCG CCCCTCTCCAGCGCAGGCTT AGGTCCCCGTTTACGAAGGG CAGGGGGAGGGCCTTCCCGC
                         HSE                                              MZF    R
-300 CGTGTCCCTACCCCTTGCAG ACGTCACTGCGGCGTGGCTG AGGGGACAGTCCTCTCAGTC TCATCAACCGTCCCCTCCCT GCCACCCCAAACGCCCACCG
```